ELSEVIER

Ceramics International 32 (2006) 339–344

CERAMICS INTERNATIONAL

www.elsevier.com/locate/ceramint

Electrical and thermal properties of $La_{0.7}Sr_{0.3}Ga_{0.6}Fe_{0.4}O_3$ ceramics

Serguei Koutcheiko *, Pamela Whitfield, Isobel Davidson

Institute for Chemical Process and Environmental Technology, National Research Council Canada, Ottawa, Ont., Canada K1A 0R6

Received 10 January 2005; received in revised form 27 January 2005; accepted 7 March 2005
Available online 11 May 2005

Abstract

Single-phase $La_{0.7}Sr_{0.3}Ga_{0.6}Fe_{0.4}O_3$ (LSGF) ceramic powder was prepared in one step at 1500 °C by solid-state reaction in air. The phase is a hexagonal (space group *R*-3*c*) at room temperature but becomes cubic at temperatures above ~600 °C. A high-density (97%) LSGF ceramic shows electrical conductivity of 4.3 S/cm ($E_a = 0.32$ eV) at 600 °C in air. The thermal expansion coefficient of LSGF changes drastically in air due to oxygen loss and phase transition. High-density LSGF ceramic is relatively stable in forming gas (8% H_2, 92% Ar). However, the powder decomposes in forming gas above 700 °C with formation of $LaSrGaO_4$. LSGF reacts with NiO at 1000 °C. The ability of LSGF to split the C–H bond in methane at intermediate temperatures has been also evaluated.

Keywords: A. Sintering; B. X-ray methods; C. Thermal properties; D. Perovskites

1. Introduction

The solid oxide fuel cell (SOFC) promises effective conversion of chemical energy to electric power with very little pollution. Strontium- and magnesium-doped $LaGaO_3$ (LSGM) is considered to be a very attractive electrolyte for moderate temperatures (500–700 °C) due to its relatively high ionic conductivity and chemical stability over wide ranges of oxygen partial pressure [1,2]. In a SOFC, both electrodes—cathode and anode—should be mixed electronic conductors and must be compatible with electrolyte in terms of thermal expansion and chemical reactivity at high temperatures [3]. It has been recently found that Fe-, Co- or Ni-doped $La(Sr)GaO_3$ perovskite oxides exhibit a high mixed conductivity. The conductivity was increased by the dopant in the following order, Co > Ni > Fe. However, only Fe-doped samples were stable under reducing atmosphere [4,5]. It was also reported that within the $La_{1-x}Sr_xGa_{0.6}Fe_{0.4}O_3$ family the composition with $x = 0.3$ exhibited the highest mixed conductivity and oxygen permeation rate [6]. The oxide ion conductivity of $La_{0.7}Sr_{0.3}Ga_{0.6}Fe_{0.4}O_3$ (LSGF) is extremely large (0.6 S/cm at 900 °C) therefore it is highly attractive as the oxygen-permeating membrane for CH_4 partial oxidation. It was reported that the LSGF membrane was stable in CH_4 atmosphere at 900–1000 °C [7]. Due to its high mixed conductivity, structural and compositional similarity with LSGM, LSGF might be an attractive electrode component for a SOFC based on LSGM-electrolyte.

We report here a synthesis and some properties of $La_{0.7}Sr_{0.3}Ga_{0.6}Fe_{0.4}O_3$ ceramics pertinent to SOFC electrode applications.

2. Experimental

The synthesis of $La_{0.7}Sr_{0.3}Ga_{0.6}Fe_{0.4}O_{3-\delta}$ (LSGF) material is quite challenging; a proper choice of raw materials and calcination temperature are very important. It was found that γ-FeOOH favored formation of LSGF free of secondary phases such as $LaSrGa_3O_7$ or $LaSrGaO_4$. It was also necessary to avoid any calcination of raw mixtures between 1100 and 1350 °C. The single-phase LSGF powder was prepared by a conventional solid-state reaction using dry La_2O_3 (99.99%, Aldrich), $SrCO_3$ (99.99%, Cerac), Ga_2O_3 (99.99%, Aldrich), and γ-FeOOH (99.9%, Aldrich). The gamma FeOOH contained 59.1% of Fe, based on TGA analysis under reducing atmosphere. Before weighing, the

* Corresponding author. Fax: +1 613 991 2384.
E-mail address: serguei.koutcheiko@nrc.ca (S. Koutcheiko).

0272-8842/$30.00.
doi:10.1016/j.ceramint.2005.03.011

La_2O_3 was calcined at 950 °C for 5 h to remove absorbed carbon dioxide. Raw materials of a desired composition were ball milled with zirconia balls in anhydrous ethanol for 48 h, dried, and cold pressed into cylindrical shapes at room temperature. The pellets were sintered at 1500 °C for 5 h on yttrium-stabilized zirconia plates; heating and cooling rates were 5 °C/min. The pellets were then crushed, ball-milled, pressed, and re-fired heated at 1500 °C for 5 h. Powder X-ray diffraction confirmed the single-phase character of the product. Finally, the pellets were crushed and ball milled; the powder was pressed again and sintered at 1550 °C for 2 h in order to get high-density (97% of X-ray density) ceramic samples. The density of polished cylindrical pellets was measured by the Archimedes method.

X-ray powder diffraction analyses were conducted with a parallel-beam, twin-mirror Bruker D8 system using Cu Kα (1.5418 Å) radiation. An Anton Paar HTK1200 high temperature stage was used to study in situ the effect of elevated temperature under different flowing atmospheres. The use of a parallel-beam geometry meant that sample displacement effects were negligible, negating the need for an internal standard. To avoid the intensity fade that can occur with a twin mirror system where there is excessive sample displacement, a contoured sample was used, with the slope perpendicular to the beam direction [8]. The heating rate used for the in situ experiments was 6 °C per minute. The samples were allowed to equilibrate for 20 min at each temperature before data collection commenced. The cell volumes were refined by the Rietveld method [9] following Topas [10]. Convolution-based peak profile fitting [11] was used during the refinements to achieve a better fit to the data.

A cylindrical pellet of diameter 5 mm and length 4 mm was selected for measurement of the thermal expansion coefficients. The measurements were performed in accordance with ASTM standard E 831. Powders of sintered samples from the same batch were loaded in a thermogravimetric analyzer for study of their thermal stability under different atmospheric conditions. Both thermal analyses were performed in air and forming gas (8% H_2–92% Ar) in the temperature range 200–900 °C with a Setaram-Evolution system; heating and cooling rate was 5°/min.

A rectangular sample 16 mm × 3 mm × 4 mm was selected for measurements of conductivity. The two ends of the bar were metallized by Pt paste and heated at 900 °C in air. Conductivity, σ (T), was measured with a Solartron 1260 impedance analyzer over a frequency range from 0.01 Hz to 1 GHz in the temperature range 100–900 °C; the measuring ac amplitude was kept at 50 mV. The lead resistance, as obtained by measuring the impedance of a blank cell, was subtracted out from all of the impedance data. The dc conductivity was measured by four-probe method. The conductivity of $La_{0.9}Sr_{0.1}Ga_{0.8}Mg_{0.2}O_{2.85}$ (LSGM) ceramics sintered at 1550 °C, 2 h (98% density) was measured as a reference.

Experiments to determine the catalytic activity for splitting C–H bond in methane were performed. LSGF-based catalysts were tested in a quartz tube flow reactor (Ø 0.5 cm). The reactor was heated in a Carbolite furnace. A certified gas mixture of CH_4 (5%) in Ar (from Air Products) was used for catalytic tests and forming gas was used as the reducing agent. The gas flow was measured by digital MKS flow meters. The product gas stream was analyzed by a QME 200 mass spectrometer. Typically 300 mg samples were placed in the reactor. Then the reactor was heated at 5 °C/min up to 900 °C in a flowing (40 cm^3/min) gas mixture of 5% CH_4 and 95% Ar.

3. Results and discussions

3.1. XRD analysis

The XRD pattern of the material prepared in two steps by calcinations at 1300 °C for 10 h and 1500 °C for 5 h is shown in Fig. 1(a). It is worth noting, that there was a small additional peak at $2\theta = 31.42°$, which could be assigned to the most intense (1 0 3) reflection of $LaSrGaO_4$ [12]. The X-ray diffraction pattern of $La_{0.7}Sr_{0.3}Ga_{0.6}Fe_{0.4}O_{3-\delta}$ prepared in one step by calcining in air at 1500 °C for 5 h, using γ-FeOOH, is shown in Fig. 1(b). The sample was single phase and all diffraction peaks could be indexed in a hexagonal R-3c structure with $a = 5.5244(8)$ Å, $c = 13.452(3)$ Å, $Z = 6$, $\rho_{X\text{-ray}} = 6.535$ g/cm^3 [13].

Fig. 2 shows the variation of the c/a ratio in hexagonal R-3c setting for LSGF as a function of temperature under air and nitrogen atmospheres. Although the LSGF is cubic at

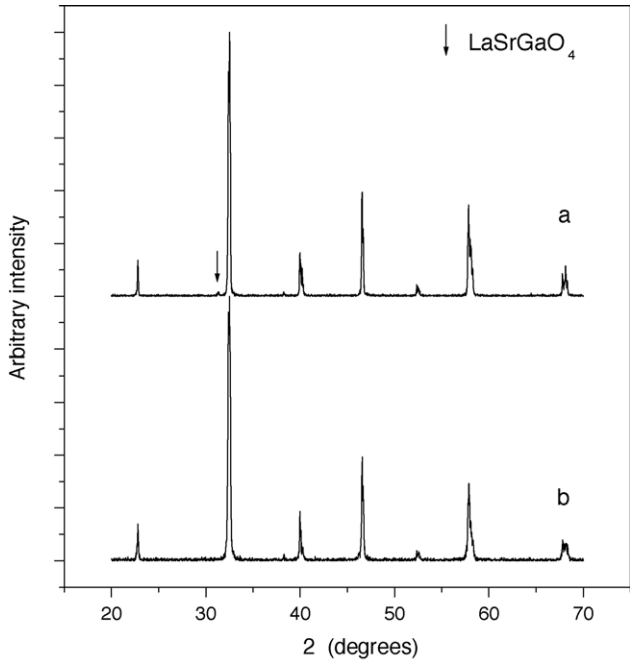

Fig. 1. X-ray diffraction patterns of LSGF powder prepared (a) in two steps at 1350 °C for 10 h and 1500 °C for 5 h and (b) in one step at 1500 °C for 5 h.

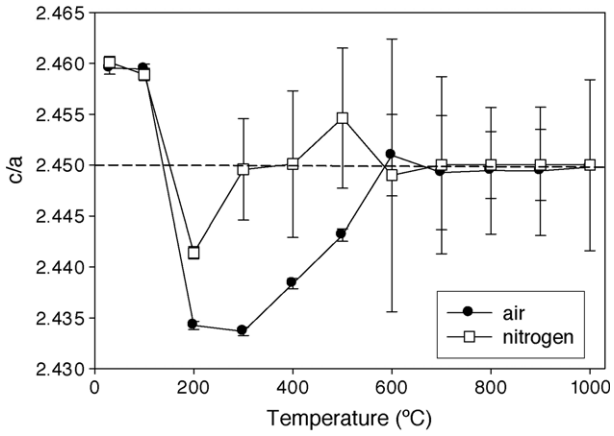

Fig. 2. Variation of *c*/*a* ratio in hexagonal *R*-3*c* cell of LSGF as a function of temperature in air and nitrogen.

high temperatures, the use of pseudo-hexagonal cell parameters makes comparisons easier across any phase transitions. It can be seen in the air plot that at ~600 °C the *c*/*a* value approaches 2.45, which corresponds to a simple cubic perovskite. Not surprisingly, once the cell is actually cubic, the errors in refining the hexagonal parameters become very large. At the same time, the splitting of the strongest perovskite peak (2θ about 32°) disappears between 500 and 600 °C; LSGF high temperature X-ray patterns are presented in Fig. 3. The temperature of 600 °C can be considered as a point where a hexagonal-to-cubic phase transition occurred in air. A more precise determination of the transition temperature was not possible with the data as the temperature increments were in 100 °C steps. A detailed investigation of phase transition in LSGF by neutron diffraction under different atmospheres is in progress. The experiments in flowing nitrogen indicated that the sample easily lost oxygen above 100 °C, probably resulting in reduction of Fe^{4+}/Fe^{3+} to Fe^{3+}/Fe^{2+}. The temperature at which the hexagonal-to-cubic phase transition occurred was lowered considerably in nitrogen (~300 °C) as indicated by

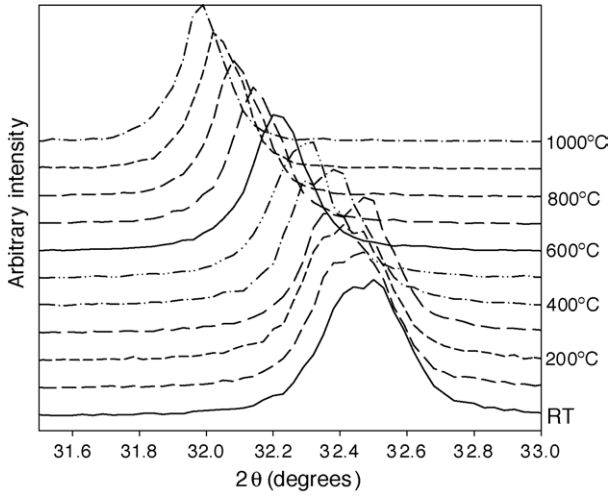

Fig. 3. XRD patterns of LSGF scanned at different temperatures.

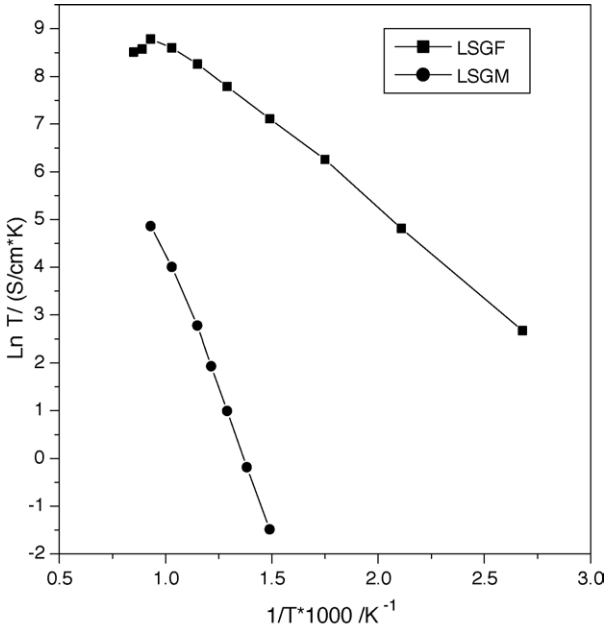

Fig. 4. Electrical conductivity of LSGM and LSGF ceramics in air.

the *c*/*a* ratio compared to air (~600 °C). The presence of Fe^{4+} in Fe-doped La(Sr)GaO_3 structure under high pO_2 atmosphere has been proven by electron spin resonance (ESR) measurements [14]. It is clear that iron reduction caused the increase in cell volume due to difference in ionic radii (for example, Fe^{4+}, Fe^{3+}, Fe^{2+} have ionic radii of 0.585, 0.645, and 0.78 Å, respectively [15]).

3.2. Electrical conductivity

Fig. 4 shows the electrical conductivity (ln σT) of LSGF ceramics (density 97%) in air as a function of 1/*T*. The conductivity of $La_{0.9}Sr_{0.1}Ga_{0.8}Mg_{0.2}O_{2.85}$ ceramics sintered at 1550 °C for 2 h (density 98%) was measured as a reference. The absolute conductivity values for LSGM and activation energy (E_a = 1.08 eV) were very close to those measured by Feng and Goodenough [1]. The LSGF ceramic has much higher electrical conductivity and lower activation energy (E_a = 0.32 eV) than LSGM does. The conductivity at 600 °C was found to be 1.8×10^{-2} and 4.3 S/cm for LSGM and LSGF, respectively. The conductivity of LSGF increases with temperature and a metal-like behavior was observed at temperatures higher than 800 °C. The generally accepted explanation for this involves the loss of oxygen from the sample at high temperatures at the expense of electron holes [7]. This is also related to the thermal reduction of Fe^{3+}.

3.3. Thermal expansion

The thermal expansion behavior in air of the ceramics investigated is presented in Fig. 5. It can be seen that expansion of LSGF depended on the density of the ceramic. Below 500 °C the difference in thermal expansion coeffi-

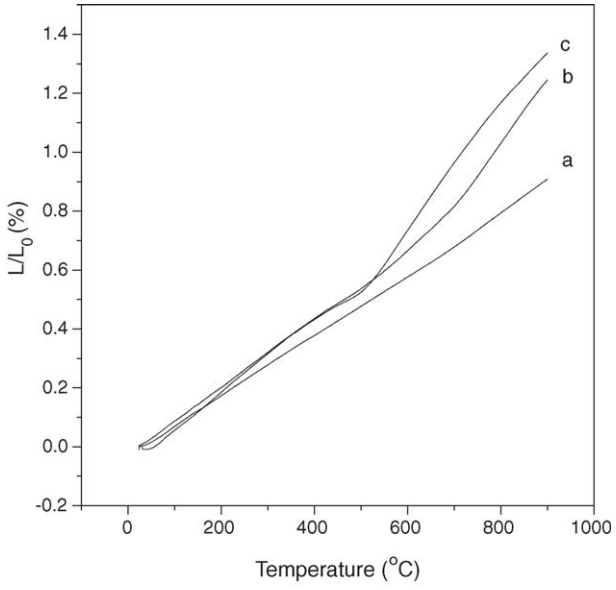

Fig. 5. Thermal expansion behavior of ceramics in air: (a) 98% density LSGM, (b) 97% density LSGF, (c) 86% density LSGF.

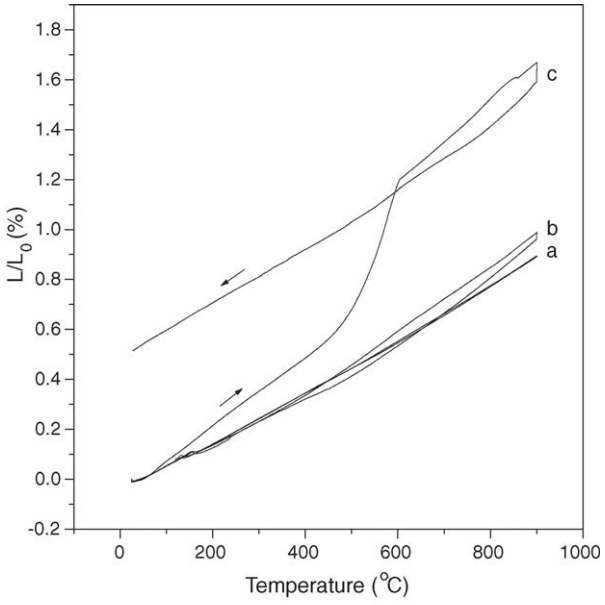

Fig. 6. Thermal expansion behavior of ceramics in forming gas: (a) 98% density LSGM, (b) 97% density LSGF, (c) 86% density LSGF.

cient (TEC) between LSGF and LSGM, which expands almost linearly with temperature, was very low. The TEC of LSGM is $10.3 \times 10^{-6}\,K^{-1}$. Above 500 °C the slope of the displacement curve for the LSGF ceramic with 86% density changed markedly, probably due to oxygen loss and phase transition; TG analysis indicated that the perovskite started to lose oxygen above 500 °C in air. It was found that TECs for LSGF (86% density) were $10.8 \times 10^{-6}\,K^{-1}$ and $\sim 19 \times 10^{-6}\,K^{-1}$ for low- and high-temperature ranges, respectively. High-density LSGF ceramic showed lower TEC in the range 500–900 °C because equilibrium with air in this case was barely achievable under experimental conditions. The TECs calculated for different temperature ranges are summarized in Table 1. The thermal behavior of ceramics under reducing conditions is shown in Fig. 6. In this case the behavior of high-density LSGF ceramic resembled the behavior of LSGM. LSGF has a TEC $11.6 \times 10^{-6}\,K^{-1}$, which is very close to that of LSGM ($10.7 \times 10^{-6}\,K^{-1}$). This means that high-density ceramic is quite stable in forming gas. Due to partial reduction, low-density ceramic showed remarkable expansion (up to 1.2%) in the temperature range 25–600 °C. However, in the cooling stage all three samples had similar TECs.

Table 1
Thermal expansion coefficients of LSGF ceramics

Temperature range (°C)	Thermal expansion coefficient ($\times 10^{-6}\,K^{-1}$)			
	Density, 6%		Density, 97%	
	Air	FG	Air	FG
200–400	10.8	12.3	11.3	–
600–900	19	–	17	–
200–900	–	11.6	–	11.6

3.4. Chemical stability

Chemical stability of LSGF under reducing atmosphere and its reactivity towards NiO were investigated. Fig. 7 shows the X-ray patterns for LSGF heated at different temperatures for 10 h in forming gas. It can be seen that

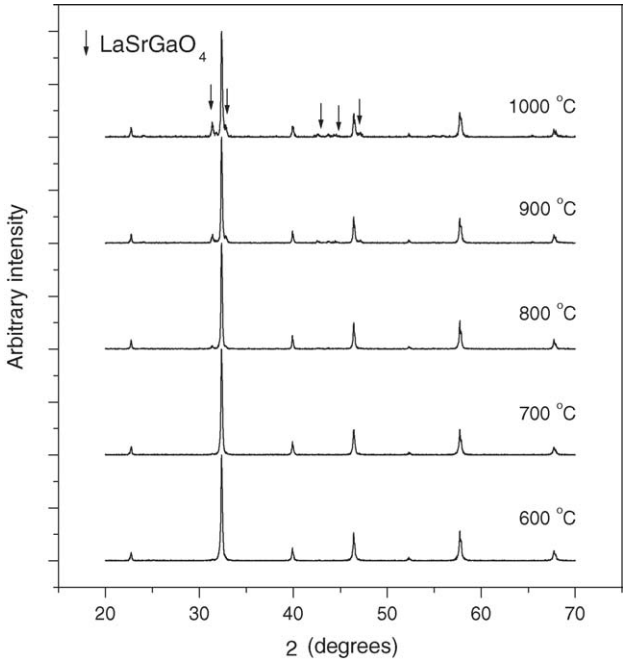

Fig. 7. X-ray diffraction patterns for LSGF powder heated in forming gas at different temperatures for 5 h.

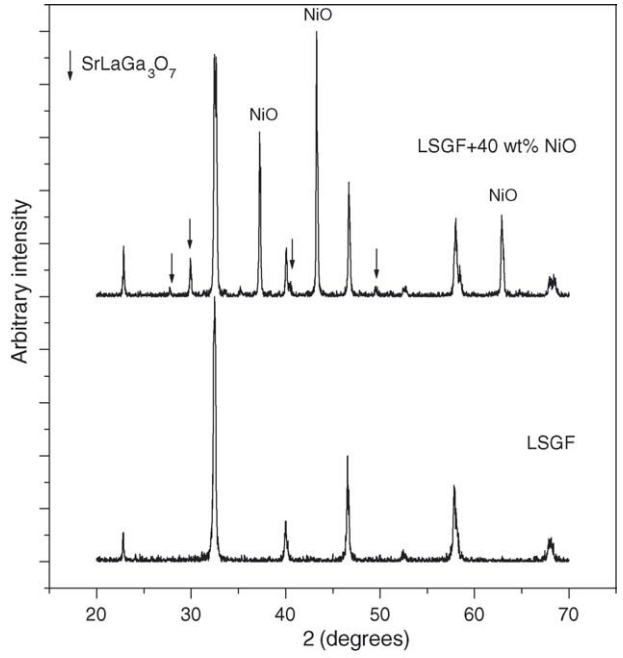

Fig. 8. X-ray diffraction pattern for LSGF–NiO mixture heated in air at 1000 °C for 10 h.

LSGF phase began to decompose above 700 °C. The second phase was $LaSrGaO_4$, probably slightly Fe-doped. The intensity of the $LaSrGaO_4$ peaks increased with temperature. It was found that at 600 °C, the LSGF ceramic heated in FG changed color from dark-brown to yellow. The yellow LSGF has a *Pm*3*m* cubic structure with $a = 3.8089$ (7) Å and unit cell volume of 59.73 Å^3, which is higher than that found at room temperature in air (pseudo-cubic cell volume 59.20 Å^3). TGA analysis in forming gas of the powder treated at 600 °C in FG showed no weight change below 700 °C. At a higher temperature, a weight loss was observed due to reduction of Fe^{3+} and sample decomposition. Fig. 8 shows the X-ray pattern of LSGF mixed with 50 wt.% of NiO and heated at 1000 °C for 10 h in air. It is clear that NiO reacted with LSGF and promoted the formation of $SrLaGa_3O_7$ as a second phase.

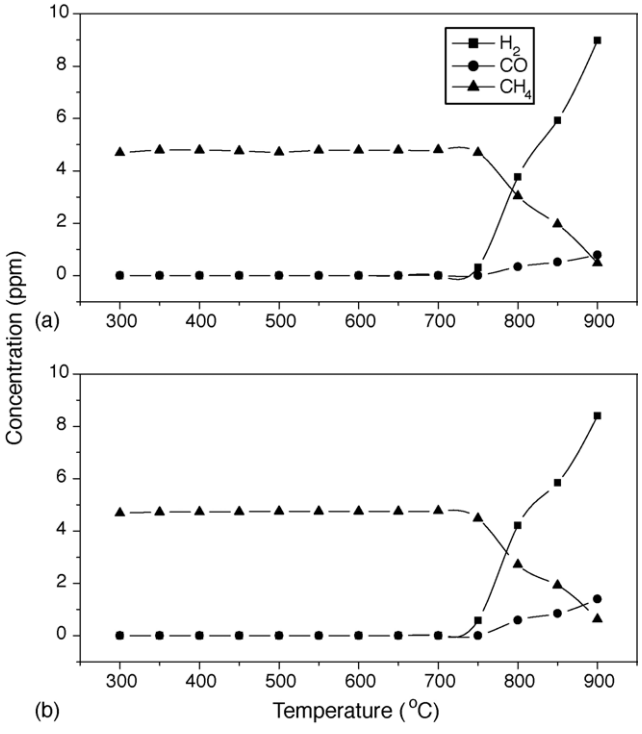

Fig. 9. Methane cracking on LSGF catalysts: (a) pre-reduced in FG and (b) as-prepared.

3.5. Catalytic test

The ability of LSGF to split the C–H bond in methane at intermediate temperatures was also tested. The test results are presented in Fig. 9. It can be seen that methane cracking started above 700 and 750 °C for as-prepared and pre-reduced samples, respectively. Our experiments showed that structural oxygen atoms play an active role in oxidizing carbonaceous species resulting in formation of CO. In case of the pre-reduced sample, the concentration of CO in the effluent gas was much lower than that for as-prepared LSGF powder. Consequently, the addition of metal catalysts such as Ni Co, Ni(Cu) will be needed in order to prepare cermet which is catalytically active in the range 500–600 °C. Unfortunately, NiO reacts with LSGF at 1000 °C (see above). Therefore, low temperature processes should be considered for metal particle deposition on the surface of LSGF.

4. Conclusions

We conclude that the single-phase composition $La_{0.7}Sr_{0.3}Ga_{0.6}Fe_{0.4}O_{3-\delta}$ can be prepared in one step by solid-state reaction at 1500 °C. It has a hexagonal perovskite structure that transforms in air into a cubic structure between 500 and 600 °C. Unfortunately, this phase transition in the $La_{0.7}Sr_{0.3}Ga_{0.6}Fe_{0.4}O_{3-\delta}$ system causes a large thermal expansion mismatch with LSGM. This may result in serious crack formation during cofiring in air. Under reducing conditions high-density LSGF and LSGM ceramics have similar TECs. LSGF ceramics are relatively stable in forming gas. However, the powder can be reduced and decomposed in forming gas with formation of $LaSrGaO_4$ above 700 °C. Based on our experiments the LSGF is catalytically active above 700 °C towards C–H bond splitting in methane and CO formation. Unfortunately, NiO reacts with LSGF at 1000 °C. Therefore, low-temperature processes should be considered for metal particle deposition on the surface of LSGF for the fabrication of catalytically active cermets for intermediate temperature SOFC.

References

[1] M. Feng, J.B. Goodenough, A superior oxide-ion electrolyte, Eur. J. Solid State Inorg. Chem. 31 (1994) 663–672.

[2] K. Huang, R.S. Tichy, J.B. Goodenough, Superior perovskite oxide-ion conductor; strontium- and magnesium-doped $LaGaO_3$: I, phase relationships and electrical properties, J. Am. Ceram. Soc. 81 (10) (1998) 2565–2575.

[3] M. Mogensen, S. Primdahl, M.J. Jorgensen, C. Bagger, Composite electrodes in solid oxide fuel cells and similar solid state devices, J. Electroceram. 52 (2000) 141–152.

[4] T. Ishihara, T. Yamada, H. Arikawa, H. Nishiguchi, Y. Takita, Mixed electroni-oxide ionic conductivity and oxygen permeating property of Fe-, Co-, or Ni-doped $LaGaO_3$ perovskite oxide, Solid State Ionics 135 (2000) 631–636.

[5] Q. Ming, M.D. Nersesyan, A. Wagner, J. Ritchie, J.T. Richardson, D. Luss, A.J. Jacobson, Y.L. Yang, Combustion synthesis and characterization of Sr-and Ga-doped $LaFeO_3$, Solid State Ionics 122 (1999) 113–121.

[6] Y. Tsuruta, T. Todaka, H. Nishiguchi, T. Ishihara, Y. Takita, Mixed electronic-oxide ionic conductor of Fe-doped $La(Sr)GaO_3$ perovskite oxide for oxygen permeating membrane, Electrochem. Solid State Lett. 4 (3) (2001) E13–E15.

[7] T. Ishihara, Y. Tsuruta, Y. Chunying, T. Tokada, H. Nishiguchi, Y. Takita, $La(Sr)Ga(Fe)O_3$ perovskite oxide as a new mixed ionic-electronic conductor for oxygen permeating membrane, J. Electrochem. Soc. 150 (1) (2003) E17–E23.

[8] P.S. Whitfield, Use of double Göbel mirrors with high temperature stages for powder diffraction—a strategy to avoid severe intensity fade, J. Appl. Cryst. 36 (2003) 926–930.

[9] H.M. Rietveld, Line profiles of neutron powder-diffraction peaks for structure refinement, Acta Cryst. 22 (1967) 151–152.

[10] Bruker-AXS, TOPAS V2.1: General Profile and Structure Analysis Software for Powder Diffraction Data. User Manual, Karlsruhe, Germany, 2003.

[11] R.W. Cheary, A.A. Coehlo, A fundamental parameters approach to X-ray line-profile fitting, J. Appl. Cryst. 25 (1992) 109–121.

[12] PDF-2 card 24–1208, International Centre for Diffraction Data, Newtown Square, PA, USA.

[13] S.E. Dann, D.B. Currie, M.T. Weller, M.F. Thomas, A.D. Al-Rawwas, The effect of oxygen stoichiometry on phase relations and structure in the system $La_{1-x}Sr_xFeO_{3-\delta}$ ($0 \leq x \leq 1$, $0 \leq \delta \leq 0.5$), J. Solid State Chem. 109 (1994) 134–144.

[14] T. Ishihara, T. Shikayama, M. Honda, H. Nishiguchi, Y. Takita, Intermediate temperature solid oxide fuel cells using $LaGaO_3$ electrolyte II. Improvement of oxide ion conductivity and power density by doping Fe for Ga site of $LaGaO_3$, J. Electrochem. Soc. 147 (4) (2000) 1332–1337.

[15] R.D. Shannon, Revised effective ionic radii and systematic studies of interatomic distances in halides and chalcogenides, Acta Cryst. A32 (1976) 751.